



## A Heavy Haze Episode in Shanghai in December of 2013: Characteristics, Origins and Implications

Qingyu Zhang<sup>1</sup>, Renchang Yan<sup>1</sup>, Juwang Fan<sup>1</sup>, Shaocai Yu<sup>1\*</sup>, Weidong Yang<sup>1</sup>, Pengfei Li<sup>1</sup>, Si Wang<sup>1</sup>, Bixin Chen<sup>1</sup>, Weiping Liu<sup>1</sup>, Xiaoyu Zhang<sup>2</sup>

<sup>1</sup> Research Center for Air Pollution and Health, College of Environmental and Resource Sciences, Zhejiang University, Hangzhou, Zhejiang 310058, China

<sup>2</sup> Department of Earth Sciences, Zhejiang University, Hangzhou, Zhejiang 310058, China

---

### ABSTRACT

As the largest Chinese city by population and the largest city proper by population in the world, Shanghai has frequently suffered the heavy haze in recent years. In this study, the observational data (PM<sub>2.5</sub>, PM<sub>10</sub>, O<sub>3</sub>, NO<sub>2</sub>, CO and SO<sub>2</sub>) at the ten urban monitoring stations in Shanghai from November 25 to December 9, 2013, were used to analyze the haze pollution. The source contributions of PM<sub>2.5</sub> in Shanghai were identified by trajectory clustering and hybrid receptor models (potential source contribution function (PSCF) and concentration weighted trajectory (CWT)). The results showed that for the whole study period, the ranges of pollutant concentrations are 2.0–635.0 μg m<sup>-3</sup> (PM<sub>2.5</sub>), 2.0–726.0 μg m<sup>-3</sup> (PM<sub>10</sub>), 1.0–139.0 μg m<sup>-3</sup> (O<sub>3</sub>), 11.0–197.0 μg m<sup>-3</sup> (SO<sub>2</sub>), 7.0–221.0 μg m<sup>-3</sup> (NO<sub>2</sub>), and 0.3–8.5 mg m<sup>-3</sup> (CO). It was found that PM<sub>2.5</sub> contributed more than 80% of PM<sub>10</sub> for the whole period except the relatively clean period in which only 45% of PM<sub>10</sub> is PM<sub>2.5</sub>. The model analyses show that clean air masses reaching at Shanghai were from the far away regions like Mongolia and Inner Mongolia with the high mean wind speed (fast air masses). On the other hand, the heavy haze air masses were mainly from the nearby industrialized and urbanized provinces with industrial cities. It was found that the formation of the extremely heavy haze from December 5 to 7 in Shanghai was mainly because of the air pollution transported from the nearby provinces (i.e., Anhui, Jiangsu, Zhejiang) and central part provinces (such as Shandong, Hebei) of eastern China. The correlation analyses among PM<sub>2.5</sub> and other pollutants show that the PM<sub>2.5</sub> formation in Shanghai is affected by the sources similar to those of CO such as combustion, industry, mobile and oxidation of hydrocarbons. Finally, the controlling strategies are discussed on the basis of this result.

**Keyword:** Air quality; Back trajectories; Cluster analysis; PSCF; CWT.

---

### INTRODUCTION

Over the past three decades, with rapid industrialization as well as vigorous urbanization, air pollution and haze weather have significantly increased in China's megacities (Chang *et al.*, 2009). As a weather phenomenon, haze has low atmospheric visibility (< 10 km) under the conditions of 80% relative humidity, and the sky becomes cloudy and bluish or yellowish (Yang *et al.*, 2012; Long *et al.*, 2014). Visibility degradation is one of the most significant features in the haze episodes. This is attributed primarily to the scattering and absorption of visible light by particulate matter (PM) in the atmosphere (Yang *et al.*, 2012). Fine particles with aerodynamic diameters of 2.5 μm and less (PM<sub>2.5</sub>) are the most effective factor for visibility impairment (Lin *et al.*, 2012;

Yang *et al.*, 2012). Haze has adverse impact on ecological systems, climate, and public health (Du *et al.*, 2011; Wang *et al.*, 2015). Moreover, the exposure to extremely high PM<sub>2.5</sub> concentrations might lead to respiratory and cardiovascular diseases as well as lung cancer (Chen *et al.*, 2012). Haze occurrence is related to chemical composition, size distribution, and mixing state of PM (Yang *et al.*, 2012; Cheng *et al.*, 2013; Long *et al.*, 2014). Haze in China mainly caused by emissions from vehicle exhausts, power plants, industrial boilers, furnaces and re-suspended dust (Fu *et al.*, 2008; Wang *et al.*, 2012). Haze formation can also be influenced by meteorological factors such as humidity, temperature, wind speed, and atmospheric pressure (Chang *et al.*, 2009; Fu *et al.*, 2010).

As the largest city by population and the largest city proper by population in China, Shanghai has undergone rapid economic development and urbanization in the past decades. Consequently, heavy air pollution and haze days frequently occur in Shanghai. The main air pollutants in Shanghai come from local emissions (i.e., vehicular, coal combustion,

---

\* Corresponding author.

E-mail address: shaocaiyu@zju.edu.cn

and fugitive dust) and regional emissions under the influence of different meteorological conditions, especially in spring and winter (Hou *et al.*, 2011; Long *et al.*, 2014). In recent years, haze events in Shanghai have been widely concerned and intensely studied (Hsu *et al.*, 2012; Cheng *et al.*, 2013; Lin *et al.*, 2014). Cheng *et al.* (2013) summarized that visual range in the Yangtze River Delta endured a reduction from 13.2 to 10.5 km from 1980 to 2000. Hsu *et al.* (2012) analyzed the global and regional trends of aerosol optical depth over land and ocean based on remote sensing products from 1997 to 2010. Fu *et al.* (2008) showed that the hourly  $PM_{2.5}$  and  $PM_{10}$  concentrations of the heavy haze days in Shanghai could reach as high as 466 and 744  $\mu\text{g m}^{-3}$  on 19 January 2007, respectively. It is found that sulfate, nitrate and ammonium are the dominant species in secondary inorganic aerosols of Shanghai (Long *et al.*, 2014), and the carbonaceous aerosols mainly emitted from the combustion sources also are important particle types in Shanghai (Hou *et al.*, 2011; Yang *et al.*, 2012). The contribution from the vehicle  $NO_x$  emissions to the aerosol formation in Shanghai exhibits an increasing trend (Wang *et al.*, 2012). In addition, the haze formations in Shanghai are related to the meteorological conditions such as relative stable synoptic situations with high RH (< 90%) and high concentrations of  $PM_{2.5}$  (Zhou *et al.*, 2014; Wang *et al.*, 2014). Meanwhile, the potential sources affecting the haze formation in Shanghai were also studied. For example, the dust aerosol in Shanghai might originate from long-range transport of dust from the upstream regions (such as Mongolia and Gobi) (Fu *et al.*, 2010; Chen *et al.*, 2012). Xiu *et al.* (2009) found that the local traffic sources from the Huabei Plain could increase mercury pollution in winter and fall in Shanghai. Wang *et al.* (2014) found that the origin of  $PM_{2.5}$  in Shanghai in late autumn might come from the upwind adjacent provinces. Based on back trajectory, Yan *et al.* (2012) found that the major contributor to polycyclic aromatic hydrocarbons (PAHs) of Shanghai might come from the southern part of China. Li *et al.* (2012) reported that major contributions to  $PM_{10}$  in Shanghai are from the northwestern sources. Cheng *et al.* (2014) reported that the open biomass burning in the adjacent provinces had significantly affected the air quality in Shanghai. Yan *et al.* (2011) reported that the mean transport contribution to the  $PM_{10}$  abundance in Shanghai reached 49% during a haze event, and this was almost the same as the contribution from the local emissions. During the world exposition 2010 with strictly controlling local emissions in Shanghai (Hao *et al.*, 2011; Huang *et al.*, 2013; Zhang *et al.*, 2013), Zhang *et al.* (2013) revealed that transports of regional pollutants affecting air quality in Shanghai mainly originated from the surrounding areas. Backward trajectories of air parcels have been applied effectively to investigate the probable source regions and preferred transport paths (Wang *et al.*, 2009; Li *et al.*, 2012; Yu *et al.*, 2014a; Li *et al.*, 2015). Potential source contribution function (PSCF) and concentration weighted trajectory (CWT) hybrid receptor models based on the back trajectories are simple and valuable tools for identifying possible source locations (Jeong *et al.*, 2011; Yu *et al.*, 2014a; Li *et al.*, 2015). Shanghai had suffered from severe haze

from December 5 to December 7, 2013, with the highest  $PM_{2.5}$  concentration of  $635 \mu\text{g m}^{-3}$ . In this study, we analyzed the air pollution ( $PM_{2.5}$ ,  $PM_{10}$ ,  $SO_2$ , CO,  $NO_2$  and  $O_3$ ) in Shanghai for the period of November 25 to December 9, 2013, using the surface and satellite observational data. To explore the possible impacts of local and regional transport sources on the formation of haze in Shanghai, the backward trajectories were computed, and the source locations and preferred paths of  $PM_{2.5}$  were further evaluated with cluster analysis, and hybrid receptor models (PSCF and CWT). Finally, the controlling strategies are discussed on the basis of these results.

## METHODOLOGY

### *Surface and Satellite Observations*

Hourly concentrations of air pollutants ( $PM_{2.5}$ ,  $PM_{10}$ ,  $O_3$ ,  $NO_2$ , CO and  $SO_2$ ) at ten urban national observation stations in Shanghai (31.22°N, 121.48°E) were measured with the standard methods ([http://www.cnemc.cn/publish/totalWebSite/0493/187/newList\\_1.html](http://www.cnemc.cn/publish/totalWebSite/0493/187/newList_1.html)) from November 25 to December 7, 2013. These observation sites include Putuo (31.238°N, 121.400°E), Shiwuchang (31.204°N, 121.478°E), Hongkou (31.301°N, 121.467°E), Xuhui (31.165°N, 121.412°E), Yangpu (31.266°N, 121.536°E), Qingpu (31.094°N, 120.978°E), Jingan (31.226°N, 121.425°E), Chuansha (31.191°N, 121.703°E), Pudongxinqiu (31.228°N, 121.533°E), and Zhangjiang (31.207°N, 121.577°E). Since the observational data at the ten urban sites are all belonged to the part of national observational network in China, the data quality and instruments meet the requirements from the China National Environmental Monitoring Center (CNEMC). The aerosol optical thickness (AOT) data at 550 nm at 6 km resolution on the ground from the satellite of Suomi National Polar-orbiting Partnership (NPP) at the level 2 were downloaded from the website (<http://ladsweb.nascom.nasa.gov/data/search.html>). Meng *et al.* (2015) show that the performance of the VIIRS aerosol product is comparable to those of MODIS retrievals and AERONET measurements on the basis of evaluation of VIIRS AOT with MODIS retrievals and AERONET measurements.

### *Back Trajectory and Cluster Analysis*

To evaluate the impact of local and regional transport sources on the formation of haze, the 48-h back trajectories arriving at the observation stations at 100 m above the ground level were computed with the NOAA Hybrid Single-Particle Lagrangian Integrated Trajectory Version 4 (HYSPPLIT4) (<http://ready.arl.noaa.gov/HYSPLIT.php>) during the study period (November 25 to December 7, 2013). The back trajectories were generated with 4-h time interval (six times per day) at starting times of –00:00, 04:00, 08:00, 12:00, 16:00 and 20:00UTC (16:00, 20:00, 00:00, 04:00, 08:00 and 12:00local times, respectively). The trajectory cluster analysis with the clustering option of Euclidean distance was performed with the software TrajStat (Wang *et al.*, 2009).

### *PSCF and CWT Methods*

The PSCF method is based on air mass residence time

allocations over specific regions in order to localize the potential sources of aerosols affecting air quality in the urban areas (Jeong *et al.*, 2011). The PSCF value can be interpreted as the conditional probability with concentrations that are larger than a given criterion value and are related to the passage of air parcels through a grid cell with this PSCF value in their paths to the receptor site (Jeong *et al.*, 2011; Mijić *et al.*, 2012; Yu *et al.*, 2014a). The higher the PSCF value, the higher the probability. In this study, PM<sub>2.5</sub> criterion is set to be 75 µg m<sup>-3</sup> based on China's national air quality standards (CNAQS) (GB3095-2012).

It is difficult for the PSCF method to distinguish the strong sources from moderate sources, while the CWT method can determine the relative significance of the potential sources (Jeong *et al.*, 2011). In the CWT method, each grid cell is assigned a weighted concentration by averaging the sample concentrations with associated trajectories that crossed the grid cell (Jeong *et al.*, 2011; Mijić *et al.*, 2012; Yu *et al.*, 2014a). The high CWT values indicate the high potential contributions to the high polluted value at the receptor site. The weighted concentration fields show concentration gradients across the potential sources, and the CWT method helps to determine the relative significance of potential sources (Mijić *et al.*, 2012).

## RESULTS AND DISCUSSION

### *Statistical Characteristics of Haze Occurrences*

To analyze the temporal variation of pollutants, the whole study period was divided into four cases: the relatively clean period 1 (November 25–30), the heavy haze period 2 (December 1–2), the haze period 3 (December 3–4), and the very heavy haze period 4 (December 5–7). Fig. 1 presents the time series of hourly pollutant concentrations (PM<sub>2.5</sub>, PM<sub>10</sub>, SO<sub>2</sub>, CO, NO<sub>2</sub>, and O<sub>3</sub>) during November 25–December 9 at the ten sites in Shanghai. For the whole study period, the mean PM<sub>2.5</sub> concentration is 157.7 µg m<sup>-3</sup> with the highest concentration of 635.0 µg m<sup>-3</sup>. For the relatively clean period 1 of November 25–30, the mean PM<sub>2.5</sub> concentration is 79.0 µg m<sup>-3</sup>, and the mean concentrations of other pollutants are 175.7 µg m<sup>-3</sup> for PM<sub>10</sub>, 27.0 µg m<sup>-3</sup> for O<sub>3</sub>, 49.4 µg m<sup>-3</sup> for SO<sub>2</sub>, 66.1 µg m<sup>-3</sup> for NO<sub>2</sub>, and 1.2 mg m<sup>-3</sup> for CO. This also indicates that 45% of PM<sub>10</sub> is PM<sub>2.5</sub> and the coarse particles (PM<sub>10</sub>–PM<sub>2.5</sub>) contributed 55% of PM<sub>10</sub> for this relatively clean period in Shanghai. The hourly NO<sub>2</sub> concentrations sometimes exceed the corresponding hourly CNAQS. On the other hand, the concentrations of O<sub>3</sub>, SO<sub>2</sub> and CO are lower than the corresponding hourly CNAQS.

For the heavy haze period 2 from December 1 to 2, average concentrations of PM<sub>2.5</sub> and PM<sub>10</sub> are 230.4 and 263.7 µg m<sup>-3</sup>, respectively. This indicates that 87% of PM<sub>10</sub> is PM<sub>2.5</sub> and the coarse particles (PM<sub>10</sub>–PM<sub>2.5</sub>) only contributed 13% of PM<sub>10</sub> for this heavy haze period in Shanghai. Average SO<sub>2</sub> and NO<sub>2</sub> concentrations are 1.5 and 2.9 times of the corresponding hourly CNAQS, respectively. In contrast, the average O<sub>3</sub> and CO concentrations are lower than the CNAQS. The average PM<sub>2.5</sub> concentration during this period is 2.3 times of the relatively clean period 1, and the concentrations of SO<sub>2</sub>, NO<sub>2</sub>, and CO are also higher than

those of the relatively clean period 1. However, the O<sub>3</sub> concentration in this period is lower than the relatively clean period 1.

For the haze period 3 from December 3 to 4, the mean PM<sub>2.5</sub> and PM<sub>10</sub> concentrations are 134.3 and 153.3 µg m<sup>-3</sup>, respectively. This shows that 88% of PM<sub>10</sub> is PM<sub>2.5</sub> and the coarse particles (PM<sub>10</sub>–PM<sub>2.5</sub>) only contributed 12% of PM<sub>10</sub> for this haze period. Of gas pollutants, only NO<sub>2</sub> concentration is 2.6 times of the CNAQS, while concentrations of O<sub>3</sub>, SO<sub>2</sub> and CO are lower than those of the CNAQS. Further, the mean PM<sub>2.5</sub> concentration is 1.7 times higher than that of the relatively clean period 1, while mean PM<sub>10</sub> concentration is lower than that of the relatively clean period 1. The concentrations of O<sub>3</sub> and NO<sub>2</sub> exceed those of the relatively clean period 1. In contrast, the concentrations of SO<sub>2</sub> and CO are lower than the relatively clean period 1. For the very heavy haze period 4 from December 5 to 7, the mean PM<sub>2.5</sub> and PM<sub>10</sub> are 246.3 and 301.5 µg m<sup>-3</sup>, respectively. This shows that 82% of PM<sub>10</sub> is PM<sub>2.5</sub> and the coarse particles (PM<sub>10</sub>–PM<sub>2.5</sub>) only contributed 18% of PM<sub>10</sub> for this very heavy haze period in Shanghai. The mean NO<sub>2</sub> concentration (101.4 µg m<sup>-3</sup>) is 2.5 times of the CNAQS. The concentrations of O<sub>3</sub>, SO<sub>2</sub>, and CO are lower than the CNAQS. It is of interest to note that except SO<sub>2</sub>, the pollutant concentrations including PM<sub>2.5</sub>, PM<sub>10</sub>, O<sub>3</sub> and CO are higher than those of the relatively clean period 1.

The AOT values from the satellite have been widely used to monitoring PM pollution. The spatial distributions of AOT at 550 nm over the eastern China in different periods are shown in Fig. 2, i.e., 11/29 (3:35 UTC), 12/2 (4:20 UTC), 12/5 (5:00 UTC), 12/6 (4:45 0UTC), and 12/9 (5:25 UTC). As can be seen, the high values of AOT (red) over the whole eastern China during the haze episodes (such as 9/6) are consistent with high PM<sub>2.5</sub> observed in Shanghai in this study.

### *Backward Trajectory and Cluster Analysis*

Secondary aerosol formation not only depends on gaseous precursors from the local emissions but also can occur during the air mass transport (Yu *et al.*, 2003; 2004; 2007a; 2008; Yu 2014; Zhang 2008; Yuan *et al.*, 2014). Meteorological conditions play a very important role in the accumulation of PM for the Yangtze River delta (YRD) (Wang *et al.*, 2015). Trajectory clustering is used in this study to identify the relationship between hourly PM<sub>2.5</sub> concentrations and transport patterns in Shanghai. The results are shown in Fig. 3 and summarized in Table 1. The percentages of trajectories for each cluster, mean PM<sub>2.5</sub> concentrations and mean wind speeds are also summarized in Table 1. For the whole period, five clusters (i.e., transport pathways) were determined: South–Southeast (S–SE), West–Northwest (W–NW), Northwest (NW), North–Northwest (N–NW), and North–Northeast (N–NE). For the relatively clean period 1 (see Table 1, and Fig. 3(b)), the cluster N–NW accounted for 21.0% air masses which originate from Mongolia across Inner Mongolia (China) before reaching at Shanghai and have long trajectories and relative low air pollutants (fast air masses, mean wind speed of 15.9 m s<sup>-1</sup>). The cluster NW accounted for 63.6% air masses which originate from Inner

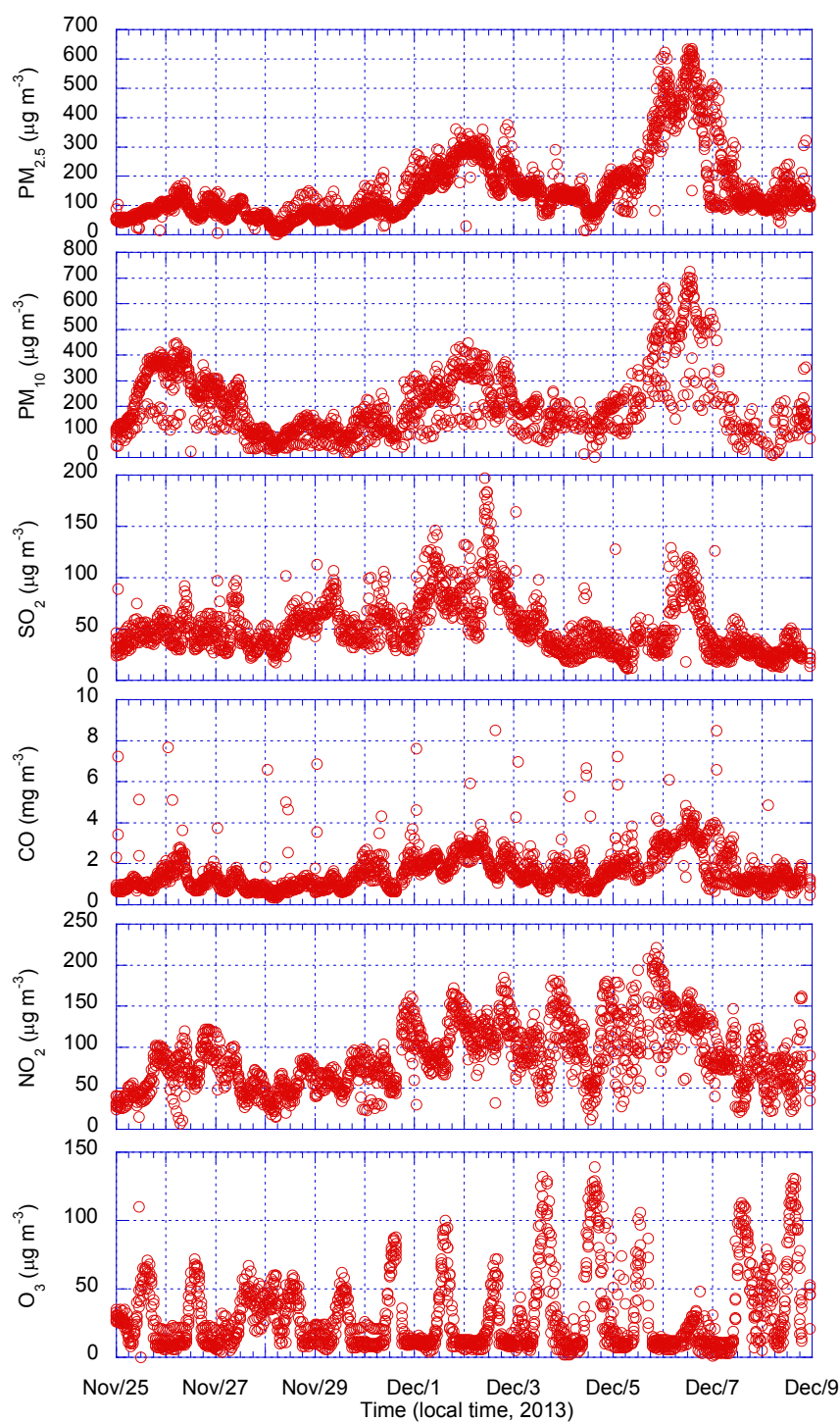


**Fig. 1.** The time series of hourly concentrations of  $\text{PM}_{2.5}$ ,  $\text{PM}_{10}$ ,  $\text{SO}_2$ ,  $\text{CO}$ ,  $\text{NO}_2$  and  $\text{O}_3$  for the period of November 25 to December 9, 2013, at the 10 sites in Shanghai city.

Mongolia (China) with the mean speed of  $7.6 \text{ m s}^{-1}$  and mean  $\text{PM}_{2.5}$  concentration of  $78.68 \text{ } \mu\text{g m}^{-3}$ . On the other hand, the cluster W–NW accounted for 15.4% air masses which come from Hebei province associated with the mean  $\text{PM}_{2.5}$  concentration of  $94.15 \text{ } \mu\text{g m}^{-3}$  exceeding slightly the CNAQS.

For the heavy haze period 2 from December 1 to 2, the only cluster W–NW account for 100% air masses which originate from Anhui and Jiangsu provinces with mean  $\text{PM}_{2.5}$

concentration of  $227.99 \text{ } \mu\text{g m}^{-3}$  (see Table 1 and Fig. 3(c)). The back trajectories of this cluster show short transport patterns with relatively low mean wind speed ( $4.7 \text{ m s}^{-1}$ ). For the haze period 3 (Table 1 and Fig. 3(d)), all trajectories can be separated into two clusters SE and W–NW. The cluster SE account for 66.1% air masses with the mean  $\text{PM}_{2.5}$  concentration of  $121.76 \text{ } \mu\text{g m}^{-3}$  and low wind speed of  $3.4 \text{ m s}^{-1}$ , and 65% of trajectories are polluted. The air

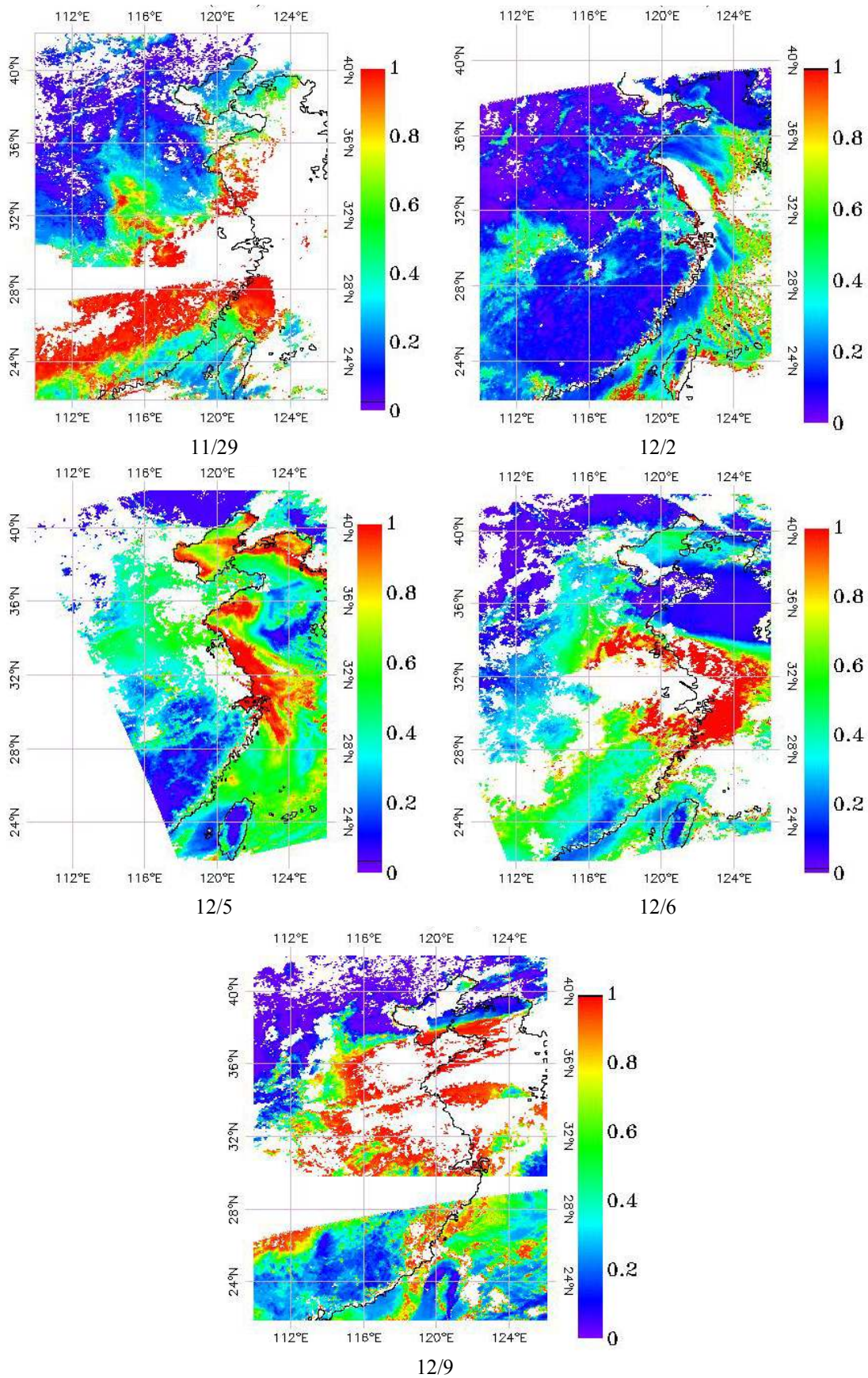


**Fig. 2.** Observations of AOT at 550 nm from the NPP satellite on 11/29 (3:35 UTC), 12/2 (4:20 UTC), 12/5 (5:00 UTC), 12/6 (4:45 UTC), and 12/9 (5:25 UTC), 2013, over the eastern China.

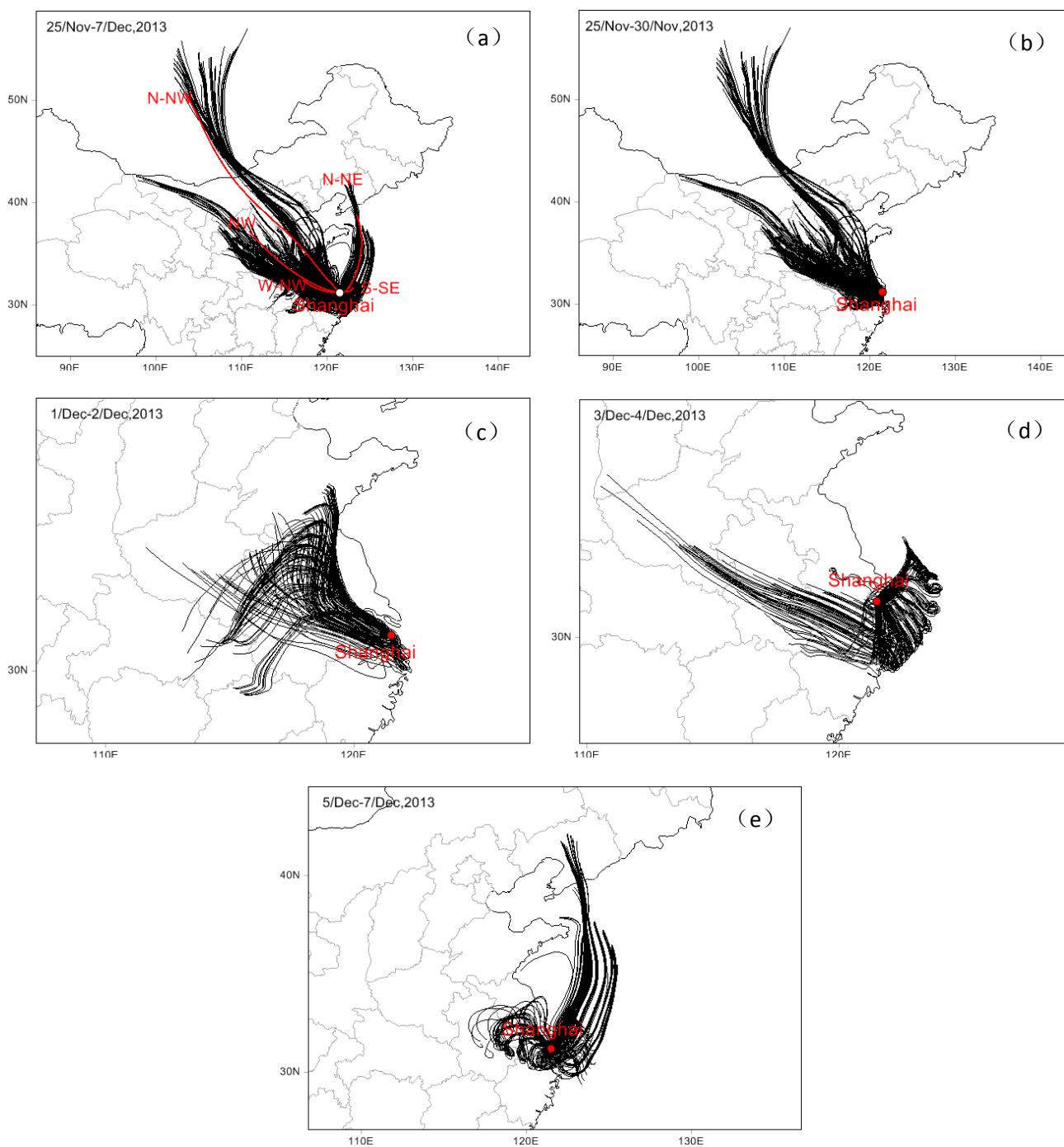


**Fig. 3.** Cluster analysis of the 48-h air mass back trajectories starting at 100 m from the 10 monitoring sites in Shanghai for the period of November 25 to December 7, 2013. (a) All back trajectories for the whole period from November 25 to December 7. The five transport pathways (clusters) are determined: S–SE (South–SouthEast), W–NW (West–NorthWest), NW (NorthWest), N–NW (North–NorthWest) and N–NE (North–NorthEast); (b) All back trajectories for the relatively clean period 1 from November 25 0:00 to November 30 23:00; (c) All back trajectories for the heavy haze period 2 from December 1 0:00 to December 2 23:00; (d) All back trajectories for the haze period 3 from December 3 0:00 to December 4 23:00; and (e) All back trajectories for the very heavy haze period 4 from December 5 0:00 to December 7 23:00 (see the explanations in text part).

masses for this cluster SE came from Zhejiang province as shown in Fig. 3(d). The cluster W–NW account for 33.9 % air masses with relative high mean  $PM_{2.5}$  concentration of  $168.25 \mu g m^{-3}$  which originate from Henan, Anhui and

Jiangsu provinces with the mean wind speed of  $5.2 m s^{-1}$ . It is of interest to note that the air masses for this cluster W–NW actually traveled to the eastern ocean first and then came back to Shanghai city as shown in Fig. 3(d).

**Table 1.** Mean concentrations of PM<sub>2.5</sub> and percentages of trajectories (The values in the parentheses are number of back trajectories) for each trajectory cluster for five cases (i.e., the whole period from November 25 to December 7, the relatively clean period 1 from November 25 0:00 to November 30 23:00, the heavy haze period 2 from December 1 0:00 to December 2 23:00, the haze period 3 from December 3 0:00 to December 4 23:00, and the very heavy haze period 4 from December 5 0:00 to December 7 23:00). The results for the polluted cases when PM<sub>2.5</sub> criterion is set to be 75  $\mu\text{g m}^{-3}$  are also presented. Mean wind speed is calculated by dividing the distance from start point to end point by traveling time (48 hours). The “Polluted Percent” is calculated on the basis of number of trajectories from the direction such as N–NW with PM<sub>2.5</sub> concentration > 75  $\mu\text{g m}^{-3}$  divided by the total trajectories from that direction

		Percent (%)	Mean PM <sub>2.5</sub> ( $\mu\text{g m}^{-3}$ )	Mean Wind Speed ( $\text{m s}^{-1}$ )	Polluted Percent (%)	Polluted Mean PM <sub>2.5</sub> ( $\mu\text{g m}^{-3}$ )
All data for the whole period	N–NW	9.7 (75)	65.4	14.5	2.7(16)	105.75
	NW	29.3 (227)	78.68	7.1	19.9(117)	102.48
	SE	15.6 (121)	142.17	3.4	19.8(116)	145.59
25/Nov–30/Nov	W–NW	33.0 (257)	222.61	4.4	41.4(243)	231.57
	N–NE	12.4 (96)	271.76	5.8	16.2(95)	274.55
	N–NW	21.0 (75)	65.40	14.5	9.1(16)	105.75
1/Dec–2/Dec	NW	63.6 (227)	78.68	7.1	66.9(117)	102.48
	W–NW	15.4 (55)	94.15	3.7	24.0(42)	102.67
	W–NW	100.0 (120)	227.99	4.7	100(120)	227.99
3/Dec–4/Dec	SE	66.1 (80)	121.76	3.4	65.2(75)	125.69
	W–NW	33.9 (41)	168.29	5.2	34.8(40)	170.65
5/Dec–7/Dec	SE	23.0 (41)	182.00	3.5	23.2(41)	182.00
	W–NW	23.0 (41)	433.54	3.3	23.2(41)	433.54
	N–NE	54.0 (96)	271.76	5.8	53.6(95)	274.55

For the very heavy haze period 4 from December 5 to 7, the whole trajectories can be separated into three clusters SE, W–NW and N–NE (see Table 1 and Fig. 3(e)). The cluster SE accounted for 23% of air masses which originated from Zhejiang province with the low wind speed of 2.5  $\text{m s}^{-1}$ . The cluster W–NW accounted for 23% of air masses with very high PM<sub>2.5</sub> mean concentration (433.54  $\mu\text{g m}^{-3}$ ) and relative low wind mean speed (5.3  $\text{m s}^{-1}$ ), originating from Anhui, and Jiangsu provinces. The cluster N–NE accounted for 54% air masses with the mean PM<sub>2.5</sub> concentration of 271.76  $\mu\text{g m}^{-3}$  and most of air masses traveled across the Yellow Sea before reaching Shanghai as shown in Fig. 3(e). The satellite observations of AOT on 12/5 and 12/6 in Fig. 2 clearly show that the whole eastern China including the Yellow Sea was significantly affected by the very heavy haze for the period and the haze over the Yellow Sea was produced by the transport of the haze from the central part (such as Shandong, Jiangsu, and Hebei provinces etc) of eastern China. This means that the very heavy haze for the cluster N–NE at Shanghai for this period was produced by the pollution sources over the central part of eastern China which traveled to the Yellow Sea first and then traveled south before reaching Shanghai.

Wang *et al.* (2015) indicated that the meteorological and atmospheric conditions with low wind speed and high RH can facilitate the accumulation of PM<sub>2.5</sub>. Peng *et al.* (2011) found that PM<sub>2.5</sub> and wind speed are the negative correlation. In this study, it was found that for different haze periods, trajectories vary with wind patterns, showing different transport paths. For the relatively clean period 1, most of the trajectories originated from Mongolia or Inner Mongolia (China) with strong or moderate wind speeds (fast air masses). For the very heavy haze period 4, air parcels to Shanghai

passed over the high emission areas of the surrounding provinces with the low wind speed (slow air masses). These results are in agreement with previous studies for Shanghai. Zhang *et al.* (2013) found that local sources and regional transport from the surrounding cities affected haze episode formation in Shanghai. Li *et al.* (2012) reported that under the winter monsoon, the northerly air flows from Hebei, Shandong, Anhui, and Jiangsu provinces carried high-concentration PM<sub>10</sub> to Shanghai. Air pollutants can travel through the short transport paths and significantly affect the air quality of the downwind areas (Yan *et al.*, 2011; Li *et al.*, 2012; Yu *et al.*, 2012a, b; Wang *et al.*, 2014; Yu *et al.*, 2014a, b).

#### Source Contributions Based on PSCF and CWT Analyses for PM<sub>2.5</sub>

The PSCF and CWT analyses provide a powerful tool for identifying the main atmospheric transport pathways influencing the receptors (Jeong *et al.*, 2011; Yu *et al.*, 2014a; Li *et al.*, 2015). As shown in Fig. 4, the areas with the high PSCF and CWT values are considered to be potential source areas. Fig. 4 showed that there were remarked differences in potential source areas for the four periods and the areas with the high PSCF and CWT values coincided with the urbanized and industrialized areas in China. For the relatively clean period 1 (see Figs 4(a), 4(e)), clean cold air masses come from Mongolia and Inner Mongolia (China), and PSCF and CWT analyses show the similar results. Some industrial cities along the transport paths, such as Jinchen (Shanxi province), Tongchuan (Shanxi province), Zhumadian (Henan province), Anqing (Anhui province), and Hangzhou (Zhejiang province) may contribute to high PM<sub>2.5</sub> concentration during the relatively clean period in Shanghai.

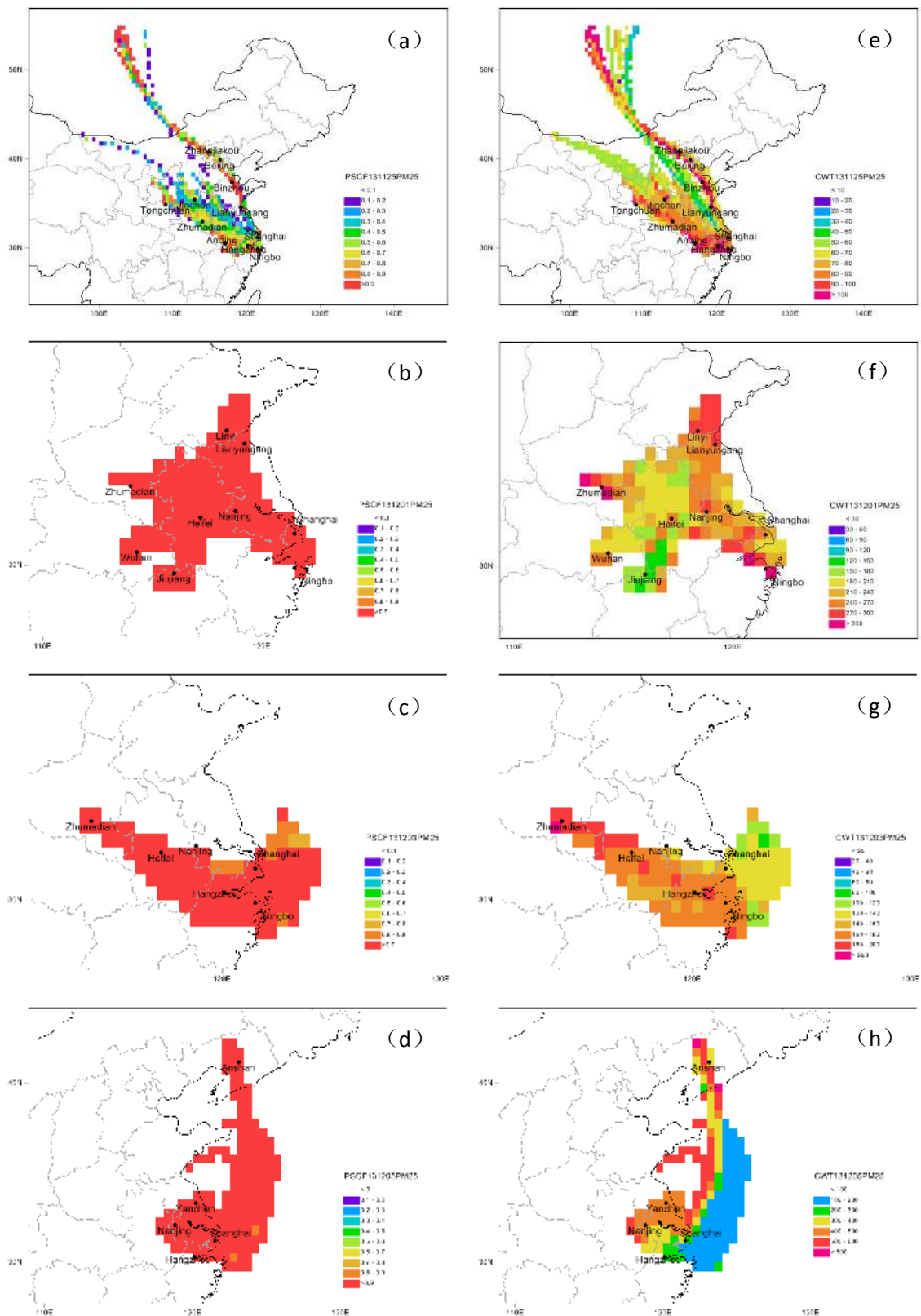


**Fig. 4.** The PSCF maps for  $PM_{2.5}$  for (a) the relatively clean period 1 from November 25 0:00 to November 30 23:00; (b) the heavy haze period 2 from December 1 0:00 to December 2 23:00; (c) the haze period 3 from December 3 0:00 to December 4 23:00; and (d) the heavy haze period 4 from December 5 0:00 to December 7 23:00. The CWT maps for  $PM_{2.5}$  ( $\mu g m^{-3}$ ) for (e) the relatively clean period 1 from November 25 0:00 to November 30 23:00; (f) the heavy haze period 2 from December 1 0:00 to December 2 23:00; (g) the haze period 3 from December 3 0:00 to December 4 23:00; and (h) the very heavy haze period 4 from December 5 0:00 to December 7 23:00.



Since the  $PM_{2.5}$  concentrations were higher than  $75 \mu g m^{-3}$  most of times for the haze periods 2, 3 and 4, almost all of the PSCF values are 1.0 as shown in Figs. 4(b), 4(c) and 4(d) for these periods. For the heavy haze period 2, the results of the CWT values (see Fig. 4(f)) show that the sources affecting high  $PM_{2.5}$  concentration in Shanghai were mainly located in the northwest of Shanghai (such as Linyi (Shandong province), Lianyungang (Jiangsu province), Zhumadian (Henan province), Hefei (Anhui province), Nanjing (Jiangsu province), Wuhan (Hubei province), Jiujiang (Jiangxi province)) and the south of Shanghai (such as Hangzhou and Ningbo (Zhejiang province)). For the haze period 3, the results of the CWT values (see Fig. 4(g)) indicate that the sources affecting high  $PM_{2.5}$  concentrations in Shanghai were mainly located in the northwest, south and west of Shanghai such as Zhumadian (Henan), Hefei (Anhui), Nanjing (Jiangsu), Hangzhou and Ningbo (Zhejiang).

For the very heavy haze period 4, the results of the CWT values (see Fig. 4(h)) show that the sources affecting the extremely high  $PM_{2.5}$  concentrations in Shanghai were mainly located in the northwest of Shanghai such as Yancheng and Nanjing (Jiangsu province). As analyzed in previous section 3.2 and shown in Fig. 2 for the satellite observations, the heavy haze over the Yellow Sea was produced by the transport of the haze from the central part (such as Shandong, Jiangsu, and Hebei provinces etc.) of eastern China. This heavy haze finally affected the formation of the very heavy haze in Shanghai as identified by the CWT values in Fig. 4(h). The Central Plains in China are the critical pollutant source regions with dense population and rapid economic development (Huang *et al.*, 2012).

Our results are consistent with the other studies. For example, Zhang *et al.* (2013) reported that air masses passing over highly polluted areas (such as Anhui, Jiangxi, Zhejiang, Shandong and Jiangsu provinces) affected air quality at the ground level in Shanghai. Wang *et al.* (2014) found that the majority of  $PM_{2.5}$  of heavy haze episode in Shanghai was partly contributed by regional transports of pollutants from the upwind adjacent provinces. Fu *et al.* (2008) indicated that at the peak of a haze episode, air masses from Lianyungang (Jiangsu province) with very high local daily concentration of  $PM_{10}$  ( $312 \mu g m^{-3}$ ) impacted the air quality at the ground level in Shanghai. Hou *et al.* (2011) also found that long-range transport of pollutants from northern and northwestern China made a significant contribution to the  $PM_{2.5}$  concentrations in Shanghai.

### **Control Strategies for Haze in Shanghai**

Understanding the relationship between potential regional sources and haze formation is necessary to control haze events. The present results demonstrate that cross-border transports of pollutants are one of important factors for determining the high  $PM_{2.5}$  levels and haze formation in Shanghai although local emission sources in Shanghai cannot be neglected as well. Local sources from industrial process and vehicle emission may also have large contribution for heavy haze episodes in Shanghai as pointed out by Wang *et al.* (2014). Fig. 5 summarized the correlation coefficients among  $PM_{2.5}$ ,  $PM_{10}$ ,  $O_3$ ,  $NO_2$ , CO and  $SO_2$  for the whole

studying period in Shanghai. As can be seen,  $PM_{2.5}$  has the strongest correlation with CO ( $r = 0.67$ ), followed by  $NO_2$  ( $r = 0.62$ ). Since CO is a long-lived tracer of human activity with well-known sources such as combustion, industry, mobile, and oxidation of hydrocarbons (Chin *et al.*, 1994; Yu *et al.*, 2006b), the significant correlation between  $PM_{2.5}$  and CO indicates that  $PM_{2.5}$  formation in Shanghai is also caused by these different emission sources. Since both mobile and industrial (mainly coal-burning) sources can emit high level of  $NO_x$ , the significant correlation between  $PM_{2.5}$  and  $NO_2$  indicates the significant contribution from both mobile and industrial sources. Heating supplied by the power grid could produce high concentrations of particles precursors such as  $SO_2$ ,  $NO_x$ , etc. The negative correlation ( $r = -0.21$ ) between  $PM_{2.5}$  and  $O_3$  indicates that when the urban activities (such as mobiles and heating) produce high concentrations of particles precursors such as  $SO_2$ ,  $NO_x$ , etc. and these high  $NO_x$  concentrations could destroy the  $O_3$  by chemical titration of NO during the nighttime (Chin *et al.*, 1994; Yu *et al.*, 2006b; Ran *et al.*, 2009). On the other hand, it was found that the severe haze event was driven to a large extent by secondary aerosol formation in China (Huang *et al.*, 2014). The development of pollution control strategies should include reduction of emissions of both primary pollutants and secondary aerosol precursors (Huang *et al.*, 2014). Our study shows that the potential sources for the heavy haze formation in Shanghai were mainly located in its adjourn provinces such as Jiangsu, Anhui and Zhejiang. Wang *et al.* (2014) also suggested that effective emission control in upwind adjacent Zhejiang and Jiangsu provinces can effectively reduce the occurrence of the haze episodes in Shanghai. As a successful example, during 2010 Shanghai World Expo, Shanghai government implemented a series of air pollution control measures for reducing emissions from local and adjacent Jiangsu and Zhejiang provinces to decrease regional transport of air pollutants to Shanghai (Huang *et al.*, 2012). The results from this study also suggest that it is necessary to implement the air pollution control measures for all industrial areas locally, regionally, even nationally in China, especially for the rapid industrial development areas in eastern China.

### **CONCLUSION**

Shanghai, as the largest Chinese city by population and the largest city proper by population in the world, has frequently suffered from severe haze. This study analyzed the characteristics of air pollution ( $PM_{2.5}$ ,  $PM_{10}$ ,  $O_3$ ,  $NO_2$ , CO and  $SO_2$ ) for the period of November 25 to December 9, 2013, on the basis of surface observations at the ten urban monitoring stations and satellite data. On the basis of the  $PM_{2.5}$  concentrations, the whole study period was separated into four periods: the relatively clean period 1 (November 25–30), the heavy haze period 2 (December 1–2), the haze period 3 (December 3–4), and the very heavy haze period 4 (December 5–7). It was found that the mean  $PM_{2.5}$  ( $PM_{10}$ ) concentrations are 79.0 (175.7), 230.4 (263.7), 134.3 (153.3) and 246.3 (301.5)  $\mu g m^{-3}$  for the relatively clean period 1, the heavy haze period 2, the haze period 3, and the very

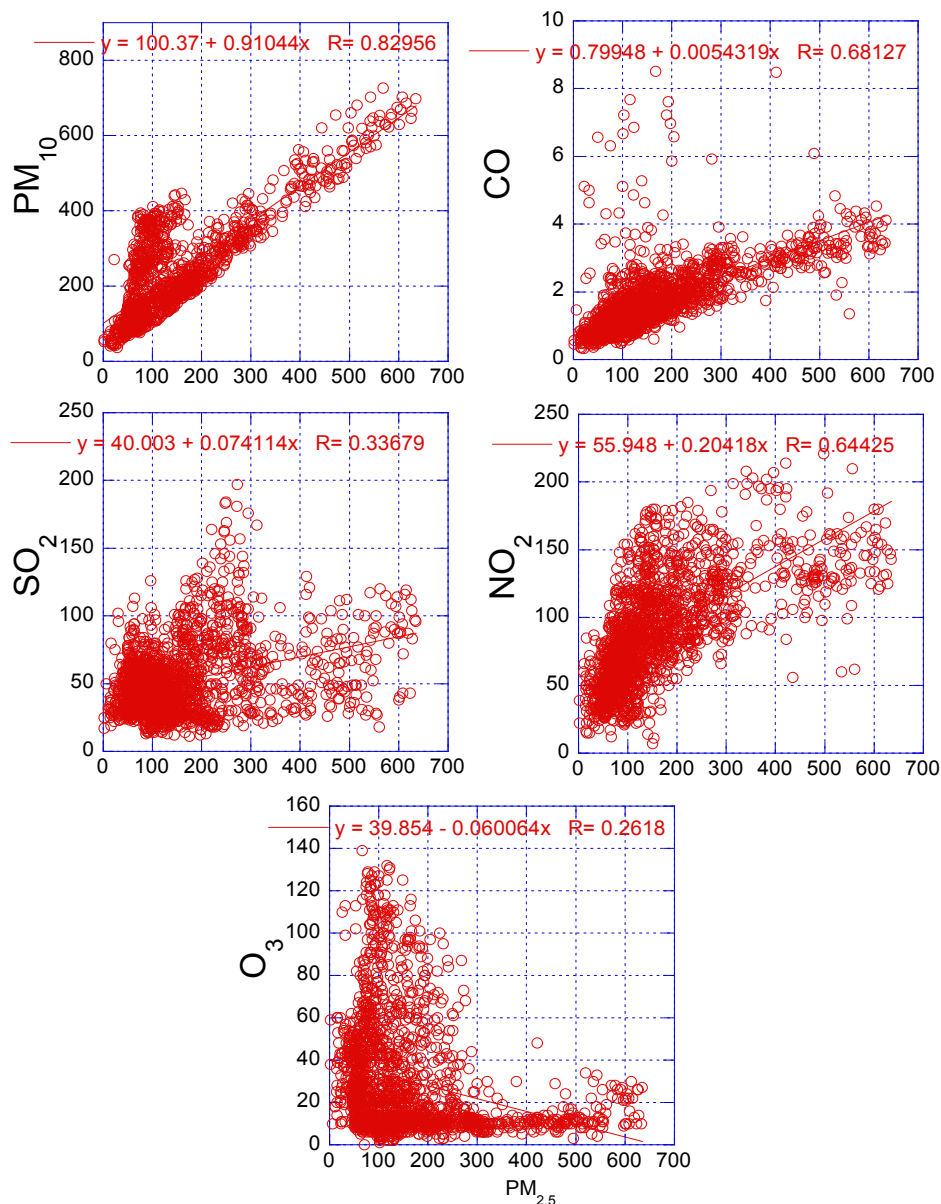


**Fig. 5.** Correlations between  $PM_{2.5}$  and other pollutants ( $PM_{10}$ , CO,  $SO_2$ ,  $NO_2$  and  $O_3$ ) for the whole studying period in Shanghai. The units for all species are  $\mu g m^{-3}$  except CO with the unit of  $mg m^{-3}$ .

heavy haze period 4, respectively.  $PM_{2.5}$  contributed more than 80% of  $PM_{10}$  for the whole period except the relatively clean period 1 in which only 45% of  $PM_{10}$  is  $PM_{2.5}$ . The results of the HYSPLIT model and receptor models show that clean air masses reaching at Shanghai were coming from the very far away regions like Mongolia and Inner Mongolia with the high mean wind speed (fast air masses). It was found that the heavy haze air masses were mainly from the nearby industrialized and urbanized provinces. It was found that the formation of the very heavy haze from December 5 to 7 in Shanghai was mainly because of the air pollution transport from the nearby provinces (i.e., Anhui, Jiangsu, Zhejiang) and central part provinces (such as Shandong, Hebei) of eastern China. The correlation analysis shows that  $PM_{2.5}$  formation in Shanghai is affected by the sources similar to those of CO such as combustion,

industry, mobile and oxidation of hydrocarbons. To improve the haze pollution in Shanghai, it is necessary to reduce emissions and air pollution in the areas, locally and regionally, as a whole to ensure blue skies and good air quality in Shanghai.

#### ACKNOWLEDGEMENTS

The part of this work is supported by the “Zhejiang 1000 Talent Plan” and Research Center for Air Pollution and Health in Zhejiang University.

#### REFERENCES

Chang, D., Song, Y. and Liu, B. (2009). Visibility Trends in Six Megacities in China 1973–2007. *Atmos. Res.* 94:

- 161–167.
- Chen, Y., Liu, Q., Geng, F., Zhang, H., Cai, C., Xu, T., Ma, X. and Li, H. (2012). Vertical Distribution of Optical and Micro-physical Properties of Ambient Aerosols during Dry Haze Periods in Shanghai. *Atmos. Environ.* 50: 50–59.
- Cheng, Z., Wang, S., Jiang, J., Fu, Q., Chen, C., Xu, B., Yu, J., Fu, X. and Hao, J. (2013). Long-term Trend of Haze Pollution and Impact of Particulate Matter in the Yangtze River Delta, China. *Environ. Pollut.* 182: 101–110.
- Cheng, Z., Wang, S., Fu, X., Watson, J.G., Jiang, J., Fu, Q., Chen, C., Xu, B., Yu, J., Chow, J.C. and Hao, J. (2014). Impact of Biomass Burning on Haze Pollution in the Yangtze River delta, China: A Case Study in Summer 2011. *Atmos. Chem. Phys.* 14:4573–4585.
- Chin, M., Jacob, D.J., Munger, J.W., Parrish, D.D. and Doddridge, B.G. (1994). Relationship of Ozone and Carbon Monoxide over North America. *J. Geophys. Res.* 99: 14565–14573
- Du, H., Kong, L., Cheng, T., Chen, J., Du, J., Li, L., Xia, X., Leng, C. and Huang, G. (2011). Insights into Summertime Haze Pollution Events over Shanghai Based on Online Water-soluble Ionic Composition of Aerosols. *Atmos. Environ.* 45:5131–5137.
- Fang, M., Chan, C.K. and Yao, X. (2009). Managing Air Quality in a Rapidly Developing Nation: China. *Atmos. Environ.* 43:79–86.
- Feng, J., Li, M., Zhang, P., Gong, S., Zhong, M., Wu, M., Zheng, M., Chen, C., Wang, H. and Lou, S. (2013). Investigation of the Sources and Seasonal Variations of Secondary Organic Aerosols in PM<sub>2.5</sub> in Shanghai with Organic Tracers. *Atmos. Environ.* 79: 614–622.
- Fu, Q., Zhuang, G., Wang, J., Xu, C., Huang, K., Li, J., Hou, B., Lu, T. and Streets, D. G. (2008). Mechanism of Formation of the Heaviest Pollution Episode ever Recorded in the Yangtze River Delta, China. *Atmos. Environ.* 42: 2023–2036.
- Fu, Q., Zhuang, G., Li, J., Huang, K., Wang, Q., Zhang, R., Fu, J., Lu, T., Chen, M., Wang, Q., Chen, Y., Xu, C. and Hou, B. (2010). Source, Long-range Transport, and Characteristics of a Heavy Dust Pollution Event in Shanghai. *J. Geophys. Res.* 115: D00K29, doi: 10.1029/2009JD013208.
- Hao, N., Valks, P., Loyola, D., Cheng, Y. and Zimmer, W. (2011). Space-based Measurements of air quality during the World Expo 2010 in Shanghai. *Environ. Res. Lett.* 6: 044004.
- Hou, B., Zhuang, G., Zhang, R., Liu, T., Guo, Z. and Chen, Y. (2011). The Implication of Carbonaceous Aerosol to the Formation of Haze: Revealed from the Characteristics and Sources of OC/EC over a Mega-city in China. *J. Hazard. Mater.* 190: 529–536.
- Hsu, N., Gautam, R., Sayer, A.M., Bettenhausen, C., Li, C., Jeong, M.J., Tsay, S.C. and Holben, B.N. (2012). Global and Regional Trends of Aerosol Optical Depth over Land and Ocean Using SeaWiFS Measurements from 1997 to 2010. *Atmos. Chem. Phys.* 12: 8037–8053.
- Hsu, Y.K., Holsen, T.M. and Hopke, P.K. (2003). Comparison of Hybrid Receptor Models to Locate PCB Sources in Chicago. *Atmos. Environ.* 37:545–562.
- Huang, K., Zhuang, G., Lin, Y., Wang, Q., Fu, J.S., Zhang, R., Li, J., Deng, C. and Fu, Q. (2012). Impact of Anthropogenic Emission on Air Quality over a Megacity - Revealed from an Intensive Atmospheric Campaign during the Chinese Spring Festival. *Atmos. Chem. Phys.* 12: 11631–11645.
- Huang, K., Zhuang, G., Lin, Y., Wang, Q., Fu, J., Fu, Q., Liu, T. and Deng, C. (2013). How to Improve the Air Quality over Megacities in China: Pollution Characterization and Source Analysis in Shanghai before, during, and after the 2010 World Expo. *Atmos. Chem. Phys.* 13: 5927–5942.
- Huang, R.J., Zhang, Y., Bozzetti, C., Ho, K.F., Cao, J.J., Han, Y., Daellenbach, K.R., Slowik, J.G., Platt, S.M., and Canonaco, F. (2014). High Secondary Aerosol Contribution to Particulate Pollution during Haze Events in China. *Nature* 514: 218–222.
- Huang, X.F., He, L.Y., Xue, L., Sun, T.L., Zeng, L.W., Gong, Z.H., Hu, M. and Zhu, T. (2012). Highly Time-resolved Chemical Characterization of Atmospheric Fine Particles during 2010 Shanghai World Expo. *Atmos. Chem. Phys.* 12: 4897–4907.
- Jeong, U., Kim, J., Lee, H., Jung, J., Kim, Y.J., Song, C.H. and Koo, J.H. (2011). Estimation of the Contributions of Long Range Transported Aerosol in East Asia to Carbonaceous Aerosol and PM Concentrations in Seoul, Korea Using Highly Time Resolved Measurements: A PSCF Model Approach. *J. Environ. Monit.* 13: 1905–1918.
- Li, M., Huang, X., Zhu, L., Li, J., Song, Y., Cai, X. and Xie, S. (2012). Analysis of the Transport Pathways and Potential Sources of PM<sub>10</sub> in Shanghai Based on Three Methods. *Sci. Total Environ.* 414: 525–534.
- Li, P., Yan, R., Yu, S.C., Wang, S., Liu, P. and Bao, H. (2015). Reinstate Regional Transport of PM<sub>2.5</sub> as a Major Cause Of Severe Haze in Beijing. *Proc. Natl. Acad. Sci. U.S.A.* 112: E2739–E2740, doi: 10.1073/pnas.1502596112.
- Lin, M., Tao, J., Chan, C.Y., Cao, J.J., Zhang, Z.S., Zhu, L.H. and Zhang, R.J. (2012). Regression Analyses between Recent Air Quality and Visibility Changes in Megacities at Four Haze Regions in China. *Aerosol Air Qual. Res.* 12: 1049–1061.
- Lin, Y., Huang, K., Zhuang, G., Fu, J.S., Wang, W., Liu, T., Deng, C. and Fu, Q. (2014). A Multi-year Evolution of Aerosol Chemistry Impacting Visibility and Haze Formation over an Eastern Asia Megacity, Shanghai. *Atmos. Environ.* 92: 76–86.
- Long, S., Zeng, J., Li, Y., Bao, L., Cao, L., Liu, K., Xu, L., Lin, J., Liu, W., Wang, G., Yao, J., Ma, C. and Zhao, Y. (2014). Characteristics of Secondary Inorganic Aerosol and Sulfate Species in Size-fractionated Aerosol Particles in Shanghai. *J. Environ. Sci.-China* 26: 1040–1051.
- Meng, F., Cao, C. and Shao, X. (2015). Spatio-temporal Variability of Suomi-NPP VIIRS-derived Aerosol Optical Thickness over China in 2013. *Remote Sens. Environ.* 163: 61–69.
- Mijić, Z., Stojić, A., Perišić, M., Rajšić, S. and Tasić, M. (2012). Receptor Modeling Studies for the Characterization of PM<sub>10</sub> Pollution Sources in Belgrade. *Chem. Ind. Chem.*

- Eng. Q.* 18: 623–634.
- Peng, G., Wang, X., Wu, Z., Wang, Z., Yang, L., Zhong, L. and Chen, D. (2011). Characteristics of Particulate Matter Pollution in the Pearl River Delta region, China: an Observational-based Analysis of two Monitoring Sites. *J. Environ. Monit.* 13: 1927–1934.
- Ran, L., Zhao, C., Geng, F., Tie, X., Tang, X., Peng, L., Zhou, G., Yu, Q., Xu, J. and Guenther, A. (2009). Ozone Photochemical Production in Urban Shanghai, China: Analysis Based on Ground Level Observations. *J. Geophys. Res.* 114: D15301, doi: 10.1029/2008JD010752.
- Wang, J., Hu, Z., Chen, Y., Chen, Z. and Xu, S. (2013). Contamination Characteristics and Possible Sources of PM<sub>10</sub> and PM<sub>2.5</sub> in Different Functional Areas of Shanghai, China. *Atmos. Environ.* 68: 221–229.
- Wang, M., Cao, C., Li, G. and Singh, R.P. (2015). Analysis of a Severe Prolonged Regional Haze Episode in the Yangtze River Delta, China. *Atmos. Environ.* 102: 112–121.
- Wang, S., Zhou, B., Wang, Z., Yang, S., Hao, N., Valks, P., Trautmann, T. and Chen, L. (2012). Remote Sensing of NO<sub>2</sub> Emission from the Central Urban Area of Shanghai (China) Using the Mobile DOAS Technique. *J. Geophys. Res.* 117: D13305, doi: 10.1029/2011JD016983.
- Wang, X., Chen, J., Cheng, T., Zhang, R. and Wang, X. (2014). Particle Number Concentration, Size Distribution and Chemical Composition during Haze and Photochemical Smog Episodes in Shanghai. *J. Environ. Sci.-China* 26: 1894–1902.
- Wang, Y., Zhang, X. and Draxler, R.R. (2009). TrajStat: GIS-based Software that Uses Various Trajectory Statistical Analysis Methods to Identify Potential Sources from Long-term Air Pollution Measurement Data. *Environ. Modell. Software* 24: 938–939.
- Wang, Y., Li, L., Chen, C., Huang, C., Huang, H., Feng, J., Wang, S., Wang, H., Zhang, G., Zhou, M., Cheng, P., Wu, M., Sheng, G., Fu, J., Hu, Y., Russell, A.G. and Wumaer, A. (2014). Source Apportionment of fine Particulate Matter during Autumn Haze Episodes in Shanghai, China. *J. Geophys. Res.* 119: 1903–1914.
- Xiu, G., Cai, J., Zhang, W., Zhang, D., Bueeler, A., Lee, S., Shen, Y., Xu, L., Huang, X. and Zhang, P. (2009). Speciated Mercury in Size-fractionated Particles in Shanghai Ambient Air. *Atmos. Environ.* 43: 3145–3154.
- Yan, L., Li, X., Chen, J., Wang, X., Du, J. and Ma, L. (2012). Source and Deposition of Polycyclic Aromatic Hydrocarbons to Shanghai, China. *J. Environ. Sci.-China* 24: 116–123.
- Yan, P., Wang, Z., Wang, X., Fu, Q. and Wang, Q. (2011). Impact of Pollutant Transport on the Air Quality of Shanghai in 2007. *SOLA* 7: 85–88.
- Yang, F., Chen, H., Du, J., Yang, X., Gao, S., Chen, J. and Geng, F. (2012). Evolution of the Mixing State of Fine Aerosols during Haze Events in Shanghai. *Atmos. Res.* 104: 193–201.
- Ying, Q., Wu, L. and Zhang, H. (2014). Local and Inter-regional Contributions to PM<sub>2.5</sub> Nitrate and Sulfate in China. *Atmos. Environ.* 94: 582–592.
- Yu, S. (2000). The Role of Organic Acids (Formic, Acetic, Pyruvic and Oxalic) in the Formation of Cloud Condensation Nuclei (CCN): A Review. *Atmos. Res.* 53: 185–5217.
- Yu, S., Saxena, V.K., Wenny, B.N., DeLuisi, J.J., Yue, G.K. and Petropavlovskikh, I.V. (2000). A Study of the Aerosol Radiative Properties Needed to Compute Direct Aerosol Forcing in the Southeastern US. *J. Geophys. Res.* 105: 24739–24749.
- Yu, S., Saxena, V.K. and Zhao, Z. (2001a). A comparison of Signals of Regional Aerosol-induced Forcing in Eastern China and the Southeastern United States. *Geophys. Res. Lett.* 28: 713–716.
- Yu, S., Zender, C.S. and Saxena, V.K. (2001b). Direct Radiative Forcing and Atmospheric Absorption by Boundary Layer Aerosols in the Southeastern US: Model Estimates on the Basis of New Observations. *Atmos. Environ.* 35: 3967–3977.
- Yu, S., Kasibhatla, P.S., Wright, D.L., Schwartz, S.E., McGraw, R. and Deng, A. (2003). Moment-based Simulation of Microphysical Properties of Sulfate Aerosols in the Eastern United States: Model Description, Evaluation and Regional Analysis. *J. Geophys. Res.* 108: 4353, doi: 10.1029/2002JD002890.
- Yu, S., Dennis, R., Bhawe, P. and Eder, B. (2004). Primary and Secondary Organic Aerosols over the United States: Estimates on the Basis of Observed Organic Carbon (OC) and Elemental Carbon (EC), and Air Quality Modeled Primary OC/EC Ratios. *Atmos. Environ.* 38: 5257–5268.
- Yu, S., Dennis, R., Roselle, S., Nenes, A., Walker, J., Eder, B., Schere, K., Swall, J. and Robarge, W. (2005). An Assessment of the Ability of 3-D Air Quality Models with Current Thermodynamic Equilibrium Models to Predict Aerosol NO<sub>3</sub><sup>-</sup>. *J. Geophys. Res.* 110: D07S13, doi: 10.1029/2004JD004718.
- Yu, S., Eder, B., Dennis, R., Chu, S. and Schwartz, S. (2006a). New Unbiased Symmetric Metrics for Evaluation of Air Quality Models. *Atmos. Sci. Lett.* 7: 26–34.
- Yu, S., Mathur, R., Kang, D., Schere, K., Eder, B. and Pleim, J. (2006b). Performance and Diagnostic Evaluations of a Real-time Ozone Forecast by the Eta-CMAQ Model Suite during the 2002 New England Air Quality Study (NEAQS). *J. Air Waste Manage. Assoc.* 56: 1459–1471.
- Yu, S., Bhawe, P.V., Dennis, R.L. and Mathur, R. (2007a). Seasonal and Regional Variations of Primary and Secondary Organic Aerosols over the Continental United States: Semi-empirical Estimates and Model Evaluation. *Environ. Sci. Technol.* 41: 4690–4697.
- Yu, S., Mathur, R., Schere, K., Kang, D., Pleim, J. and Otte, T.L. (2007b). A Detailed Evaluation of the Eta-CMAQ Forecast Model Performance for O<sub>3</sub>, Its Related Precursors, and Meteorological Parameters during the 2004 ICARTT Study. *J. Geophys. Res.* 112:D12S14, doi: 10.1029/2006JD007715.
- Yu, S., Mathur, R., Schere, K., Kang, D., Pleim, J., Young, J., Tong, D., McKeen, S. and Rao, S. (2008). Evaluation of Real-time PM<sub>2.5</sub> Forecasts and Process Analysis for PM<sub>2.5</sub> Formation over the Eastern U.S. Using the Eta-CMAQ Forecast Model during the 2004 ICARTT Study. *J. Geophys. Res.* 113: D06204, doi: 10.1029/2007JD009226.

- Yu, S. and Zhang, Y. (2011). An Examination of the Effects of Aerosol Chemical Composition and Size on Radiative Properties of Multi-Component Aerosols. *Atmos. Climate Sci.* 1: 19–32, doi: 10.4236/acs.2011.12003.
- Yu, S., Mathur, R., Pleim, J., Pouliot, G., Eder, B., Schere, K., Wong, D., Gilliam, R. and Rao, S. (2012a). Comparative Evaluation of the Impact of WRF/NMM and WRF/ARW Meteorology on CMAQ Simulations for PM<sub>2.5</sub> and its Related Precursors during the 2006 TexAQS/GoMACCS Study. *Atmos. Chem. Phys.* 12: 4091–4106, doi: 10.5194/acp-12-4091-2012.
- Yu, S., Mathur, R., Pleim, J., Pouliot, G., Eder, B., Schere, K., Wong, D., Gilliam, R. and Rao, S. (2012b). Comparative Evaluation of the Impact of WRF-NMM and WRF-ARW Meteorology on CMAQ Simulations for O<sub>3</sub> and Related Species during the 2006 TexAQS/GoMACCS Campaign. *Atmos. Pollut. Res.* 3: 149–162.
- Yu, S. (2014). Water Spray Geoengineering to Clean Air Pollution for Mitigating Haze in China's Cities. *Environ. Chem. Lett.* 12: 109–116.
- Yu, S., Zhang, Q., Yan, R., Wang, S., Li, P., Chen, B., Liu, W. and Zhang, X. (2014a). Origin of Air Pollution during a Weekly Heavy Haze Episode in Hangzhou, China. *Environ. Chem. Lett.* 12:543–550.
- Yu, S., Mathur, R., Pleim, J., Wong, D., Gilliam, R., Alapaty, K., Zhao, C. and Liu, X. (2014b). Aerosol Indirect Effect on the Grid-scale Clouds in the Two-way Coupled WRF-CMAQ: Model Description, Development, Evaluation and Regional Analysis. *Atmos. Chem. Phys.* 14:11247–11285, doi: 10.5194/acp-14-1-2014.
- Yu, S., Alapaty, K., Mathur, R., Pleim, J., Zhang, Y., Nolte, C., Eder, B., Foley, K. and Nagashima, T. (2014c). Attribution of the United States “Warming Hole”: Aerosol Indirect Effect and Precipitable Water Vapor. *Sci. Rep.* 4: 6929, doi: 10.1038/srep06929.
- Yuan, Q., Yang, L., Dong, C., Yan, C., Meng, C., Sui, X. and Wang, W. (2014). Temporal Variations, Acidity, and Transport patterns of PM<sub>2.5</sub> Ionic Components at a Background Site in the Yellow River Delta, China. *Air Qual. Atmos. Health* 7: 143–153.
- Zhang, M., Chen, J., Chen, X., Cheng, T., Zhang, Y., Zhang, H., Ding, A., Wang, M. and Mellouki, A. (2013). Urban Aerosol Characteristics during the World Expo 2010 in Shanghai. *Aerosol Air Qual. Res.* 13: 36–48.
- Zhang, Y. (2008). Online-coupled Meteorology and Chemistry Models: History, Current Status, and Outlook. *Atmos. Chem. Phys.* 8: 2895–2932, doi: 10.5194/acp-8-2895-2008.
- Zhou, G., Yang, F., Geng, F., Xu, J., Yang, X. and Tie, X. (2014). Measuring and Modeling Aerosol: Relationship with Haze Events in Shanghai, China. *Aerosol Air Qual. Res.* 14: 783–792.

Received for review, April 23, 2015

Revised, July 15, 2015

Accepted, August 12, 2015